

A window-based accelerating algorithm for SDA integration

YU Bao-chu^{*1,2}, YU Qing-jun³, YU Tie-jun³, TANG Zhen-an³

- (1. State Key Laboratory of Structural Analysis for Industrial Equipment, Dalian University of Technology, Dalian 116024, China;
2. School of Civil Engineering, Dalian Ocean University, Dalian 116023, China;
3. School of Electronic Science and Technology, Dalian University of Technology, Dalian 116024, China)

Abstract: Spectral domain analysis (SDA) is presented for solving complex propagation constant of on-chip multi-layer interconnects. As SDA is a full wave solution and is usually computational expensive, a novel bell-shaped window function is introduced to speed up the integral equation (IE). This novel bell-shaped window function has low-pass-filter feature in the spectral domain. Also it has simple closed-form formula which favorites the computational complexity. Based on this window's special feature research, a new accelerating algorithm is derived to speed up the SDA integration. Both the accuracy and the speed of the proposed algorithm are proved to be very promising.

Key words: spectral domain analysis (SDA); transmission line or interconnect; substrate loss; windows function; low-pass-filter window

0 Introduction

The design of high performance IC systems requires accurate high frequency analysis of interconnects. Frequency dependence analysis of interconnect or transmission line, especially the on-chip interconnect with substrate loss plays an important role in the chip signal integrity. In the silicon-based chip design, due to the loss substrate's collecting and redistributing of the digital switching noise, mixed signal chip design faces serious challenge. Spectral domain analysis or approach (SDA), which is a standard full-wave method^[1], is proposed here to do the on-chip interconnect analysis. However, the traditional SDA is very time-consuming due to the infinity integration of the system matrix's

entries in the spectral domain (SD). To overcome this difficulty, new numerical technique is needed to speed up SDA. Window function accelerated techniques are widely used in the signal processing and other applications. In fact, the concept of using window accelerated technique to speed up the integration itself is not a new one, but how to compose the appropriate window function, how to derive the acceleration algorithm is a very creative process in the SDA. In Lits. [2, 3], a 2-dimensional low-pass-filter window (LPFW) is successfully used to speed up the layered Green's function calculation. Here, this paper will introduce another new 1-dimensional LPFW and derive its spectral closed-form formulation. Based on this new window, a novel accelerating algorithm will be

Received by: 2010-01-10; Revised by: 2011-12-05.

Supported by: Key Research Project of Liaoning Province Bureau of Science and Technology (Grant No. 2008217004); China's Post-Doctoral Science Fund (Grant No. 200704111071).

Corresponding author: YU Bao-chu* (1974-), Male, Doc., Assoc. Prof., E-mail: baochuyu@student.dlut.edu.cn.

derived to speed up the traditional SDA integration calculation. The approach used here is also useful for other applications, e. g. , how to determine the earthquake destructive capability for its first few arrived shocking waves during the rupture.

1 SDA and its problems

1.1 SDA introduction

Fig. 1 shows the considering problem which is a multi-layered interconnects' cross section. Interconnect width is noted as " W ", while its thickness is noted as " t ". Each dielectric layer is defined as homogenous and is specified by $\epsilon_i, \mu_i, \sigma_i$. For a real silicon on-chip interconnect, it usually consists of a ground plane with a few hundred micron-meters thick loss substrate layer and then a very thin oxide layer which separates the first metal layer and the loss substrate. Here assuming the electromagnetic (EM) wave propagates in the x direction and a factor $e^{j\omega t - jk_x x}$ is suppressed in the later formula derivation. Complex propagation constant ($k_x = \beta - j\alpha$) is the solved object which represents the EM wave speed and also its attenuation information. With the Green's function's^[3,4] taking care of the substrate, layered dielectric and ground plane's effects, the integration equation can be generated only on the metal interconnect strip surface. The electric field on the metal strip surface can be expressed in terms of Green's function as

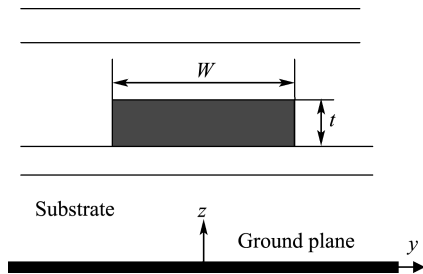


Fig. 1 Cross section of the multi-layered interconnect

$$\mathbf{E} = \int \mathbf{G} \cdot \mathbf{J} dr' \quad (1)$$

Where \mathbf{G} is the multi-layer electric field Dyadic Green's function; \mathbf{J} is the current distribution

on the metal strip, which can be expressed in terms of the basis functions of J_{xi}, J_{yj} , they are

$$\begin{aligned} J_x &= \sum_{i=0}^{N-1} C_i J_{xi} \\ J_y &= \sum_{j=0}^{M-1} D_j J_{yj} \end{aligned} \quad (2)$$

Metal strip with thickness of t can be considered as a complex resistive thin film with the effective surface resistance Z_s . On the strip surface, the boundary condition is

$$\hat{\mathbf{n}} \times \mathbf{E} = \hat{\mathbf{n}} \times (Z_s \mathbf{J}) \quad (3)$$

Following the SDA standard procedure in spectral domain^[1,5], multiplying the each current basic function J_{xi}, J_{yj} at both sides of Eq. (3); doing the integration in the corresponding support of the basic function of J_{xi}, J_{yj} , and transferring the integration into spectral domain, then system equation is arrived as follows:

$$\begin{pmatrix} \mathbf{Z}_{xx} & \mathbf{Z}_{xy} \\ \mathbf{Z}_{yx} & \mathbf{Z}_{yy} \end{pmatrix} \begin{pmatrix} \mathbf{C}_i \\ \mathbf{D}_j \end{pmatrix} = \mathbf{0} \quad (4)$$

where $\mathbf{C} = (\mathbf{C}_i \ \mathbf{D}_j)^T$ is the current expansion coefficient in Eq. (2). $\mathbf{Z} = \begin{pmatrix} \mathbf{Z}_{xx} & \mathbf{Z}_{xy} \\ \mathbf{Z}_{yx} & \mathbf{Z}_{yy} \end{pmatrix}$ is the system matrix and its sub-matrix $\mathbf{Z}_{x(y)x(y)} = (Z_{x(y)x(y)}^{ij})$ and its entry is obtained as:

$$Z_{pq}^{ij} = \int_{-\infty}^{\infty} \tilde{G}_E^{pq}(k_x, k_y) \tilde{J}_{qj}(k_y) \tilde{J}_{pi}(k_y) dk_y \quad (5)$$

Where $p, q = x, y$. Dyadic Green's function \tilde{G}_E can be obtained in SD by potential Green's functions^[3,4]. For the diagonal terms in the system matrix, matrix entry in Eq. (5) needs to be updated to consider the metal loss,

$$Z_{pp}^{ii} = Z_{pp}^{ii} - \int_{-\infty}^{\infty} Z_s \tilde{J}_{qi}(k_y) \tilde{J}_{pi}(k_y) dk_y \quad (6)$$

Complex propagation constant $k_x = K_{x0} = \beta - j\alpha$ is obtained by solving

$$\|\mathbf{Z}\| = 0 \quad (7)$$

Usually Eq. (7) can be solved with Newton-Raphson iteration. Current distribution $\mathbf{C} = (\mathbf{C}_i \ \mathbf{D}_j)^T$ on the strip can be determined in a least square sense from Eq. (4) after K_{x0} is obtained.

1.2 SDA problems

SDA is a full wave solution in which almost all the EM issues in interconnect are considered

and therefore, it is a very accurate approach. Also as the operation is done in the spectral domain, the complicate Green's function calculation in the spatial domain is avoided. However, SDA faces a serious challenge. It is extremely time-consuming to calculate the infinity integration shown in Eqs. (5), (6). This can be explained as follows. Usually, basis functions in Eq. (2) are given as:

$$J_{xi}(y) = \begin{cases} 1/W; & y_{1i} \leq |y| < y_{2i} \\ 0; & \text{otherwise} \end{cases} \quad (8)$$

$$J_{yj}(y) = \frac{\sin(2(j+1)\pi y/W)}{W \sqrt{1-(2y/W)^2}}$$

where $y_{1i} = y_i - r_i$, $y_{2i} = y_i + r_i$, $y_i = (l_i + l_{i+1})/2$, $r_i = (l_{i+1} - l_i)/2$, $l_0 = 0$, $l_N = W/2$, $l_i = l_{i+1} - b^{N-i-1}d_y$, $d_y = 0.5W(1-b)/(1-b^N)$, $i = 0, 1, \dots, N-1$, $j = 0, 1, \dots, M-1$. W is the strip width, $b > 1$ is the non-uniform discretization factor. In spectral domain, \tilde{J}_{xi} , \tilde{J}_{yj} can be obtained as:

$$\tilde{J}_{xi}(k_y) = \frac{4}{Wk_y} \cos k_y y_i \sin k_y r_i \quad (9)$$

$$\tilde{J}_{yj}(k_y) = \frac{\pi}{4j} [J_0(|P+Q|) - J_0(|P-Q|)] \quad (10)$$

Where J_0 is the zero order Bessel function, $P = 0.5Wk_y$, $Q = (j+1)\pi$. Eqs. (9), (10) show that \tilde{J}_{xi} , \tilde{J}_{yj} oscillate fastly and decay slowly. Also \tilde{G}_{pq} usually varies fastly and decays slowly especially at higher frequency with bigger number of layers. As \tilde{J}_{xi} , \tilde{J}_{yj} and \tilde{G}_{pq} are all slowly decaying and fastly oscillating functions, this leads to the longer integration interval with densely sampling points in the integration of Eq. (5) and Eq. (6) which makes the calculation very expensive. That is the main issue SDA faces.

2 Window function and its fast algorithm

2.1 Motivation

To speed up Eqs. (5), (6), one can shorten the integral interval or reduce the sampling points' number. This paper is focusing on how to shorten the integral interval. A new window function named "w" is designed to do so.

If "w" decays very fast, and if "w" multiples the integral kernel in Eqs. (5), (6), then the new integral kernel should decay fast because the "w" decays fast. To reach this goal the "w" must decay very fast in the spectral domain, and in the mathematical point of view, "w" must have a compact supporting and must be very smooth in the spatial domain, so its spectral domain (SD) component is a low-pass-filter window (LPFW) and decays fast. LPFW indicates that the low spectral components are filtered in the integration while the high spectral components are phased out.

Applying theorem

$$F = g \otimes f = \int_{-\infty}^{\infty} \tilde{g}(k_y) \tilde{f}(k_y) e^{-jk_y y} dk_y$$

and keeping this in mind to change Eq. (5) as the following:

$$Z_{pq}^{ij} \otimes w = \int_{-\infty}^{\infty} \tilde{Z}_{pq}^{ij}(k_x, k_y) \tilde{w}(k_y) e^{-jk_y y} dk_y \quad (11)$$

If \tilde{w} decays very fast, then the integral interval in the right side of Eq. (11) will be shortened dramatically. However, the left side of Eq. (11) is not Z_{pq}^{ij} as stated in Eq. (5), but a convolution of Z_{pq}^{ij} with the window of "w". To recover the value of Z_{pq}^{ij} from the convolution, Taylor series are used in the left side of Eq. (11) to expand Z_{pq}^{ij} at some fixed points as follows:

$$Z_{pq}^{ij} \otimes w \approx \int \left(Z_{pq}^{ij}(y_0) + \frac{d(Z_{pq}^{ij}(y_0))}{dy} (y - y_0) \right) \times w(\tau - y) d\tau \quad (12)$$

The second term in the integral of Eq. (12) can be chosen symmetrically and is 0, so one can finally obtain the following:

$$Z_{pq}^{ij} \otimes w \approx M_0 Z_{pq}^{ij} \quad (13)$$

Combining Eq. (11) and Eq. (13) to get the fast algorithm:

$$Z_{pq}^{ij} = \frac{1}{M_0} \int_{-\infty}^{\infty} \tilde{Z}_{pq}^{ij}(k_x, k_y) \tilde{w}(k_y) e^{-jk_y y} dk_y \quad (14)$$

Where $M_0 = \int w(\tau) d\tau$ is called the first order moment of "w", which is the integrated area under the curve of "w".

2.2 Window function

How to construct the appropriate "w" is the key point to make sure the fast algorithm's

success. According to the required properties of "w", design it as:

$$w(y) = \begin{cases} [1 - (y/a)^2]^m; & |y| \leq a \\ 0; & \text{otherwise} \end{cases} \quad (15)$$

Where m is the order of "w", a is the compact support of "w". Its SD component, \tilde{w} , can be derived as:

$$\tilde{w}(k_y) = \begin{cases} 4a \left(\frac{\sin d}{d^3} - \frac{\cos d}{d^2} \right); & m = 1 \\ \frac{16a}{d^3} \left(\frac{3-d^2}{d^2} \sin d - \frac{3}{d} \cos d \right); & m = 2 \end{cases} \quad (16)$$

where $d = k_y a$ and w' 's first moment is derived as:

$$M_0 = \begin{cases} 4a/3; & m = 1 \\ 16a/15; & m = 2 \end{cases} \quad (17)$$

2.3 Fast algorithm

The fast algorithm Eq. (14) requires \tilde{Z}_{pq}^{ij} but there is only Z_{pq}^{ij} in Eq. (5), so here Z_{xx}^{ij} is used as an example to show how to derive the fast algorithm. In Eq. (5), after doing some derivation one can get

$$Z_{xx}^{ij} = \langle \tilde{G}_E^{xx} \tilde{J}_{xj}, \tilde{J}_{xi} \rangle = \frac{2}{W} \sum_{k=0}^7 (-1)^k g_{ijk}^{xx} \quad (18)$$

Where

$$g_{ijk}^{xx} = \int_{-\infty}^{\infty} \tilde{G}_E^{xx} \frac{1}{k_y^2} e^{ik_y Y_{ijk}} dk_y = \int_{-\infty}^{\infty} \tilde{g}_{ijk}(\zeta) e^{-j\zeta} d\zeta \quad (19)$$

and $k=0,1,2,\dots,7$.

$$\begin{aligned} Y_{ij0} &= l_{j+1} + l_i; Y_{ij1} = l_{j+1} + l_{i+1} \\ Y_{ij2} &= l_{j+1} - l_{i+1}; Y_{ij3} = l_{j+1} - l_i \\ Y_{ij4} &= l_j + l_{i+1}; Y_{ij5} = l_j - l_{i+1} \\ Y_{ij6} &= l_j - l_i; Y_{ij7} = l_j + l_i \end{aligned} \quad (20)$$

To speed up Eq. (19), applying Eq. (11) and denoting $y=Y_{ijk}$, $g(y)=g_{ijk}(Y_{ijk})$, one has

$$g(y) \otimes w(y) = 2 \int_0^{\infty} \tilde{g}_{ijk}(K_{x0}, k_y) \tilde{w}(k_y) \times \cos(k_y y) dk_y \quad (21)$$

For the left side in Eq. (21), there is

$$g(y) \otimes w(y) = \int_{-\infty}^{\infty} g(x) w(y-x) dx \approx g(y) M_0 \quad (22)$$

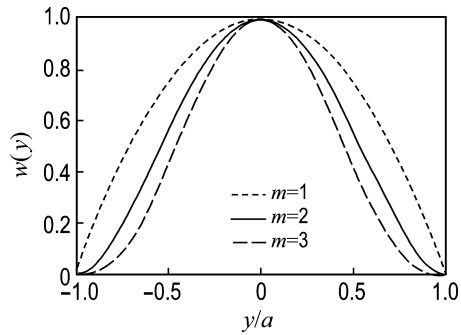
Combining Eq. (21) with Eq. (22), the fast algorithm for $g(y)=g_{ijk}(Y_{ijk})$ can be finally derived as follows:

$$g(y) \approx \frac{2}{M_0} \int_0^{\infty} \tilde{g}_{ijk}(K_{x0}, k_y) \tilde{w}(k_y) \cos(k_y y) dk_y \quad (23)$$

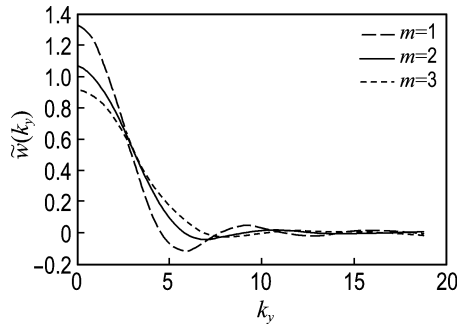
Similar to Z_{xx}^{ij} , other entries in Eqs. (5)-(6) also can be accelerated by the window-based algorithm.

3 Numerical experiments

Check window "w" itself first. Fig. 2 shows the window function both in the spatial and spectral domain. One can see that in the spatial domain it is very smooth. The bigger the m in Eq. (15) is, the smoother the window function in the spatial domain is. In this sense, naming m as the order of the window function, cases where $m > 1$ are referred to the higher order window functions. Also from Fig. 2 one can see that if the order is high, the window's spectral component $\tilde{w}(k_y)$ in Eq. (16) will be more complicated and decay faster. Decaying fast is the preferred feature, but too complicated $\tilde{w}(k_y)$ is not wanted because it will slow down the calculating speed in Eq. (14). So in this study, many m values are tried, but only $m=1, 2, 3$ are used in the final calculation. The distribution of the window function in both domains in Fig. 2 shows that "w" is well constructed with a very



(a) spatial domain



(b) spectral domain

Fig. 2 Window functions

deep descent feature in the higher spectral domain. The bigger the order m is, the smoother " w " is and the faster \tilde{w} decays.

Shown in Eq. (23), \tilde{w}' 's decaying determines the fast algorithm's gain respective to the traditional SDA. When focusing on the speed gain by using window-based acceleration, define the gain ratio as

$$X = L_d/L_w \quad (24)$$

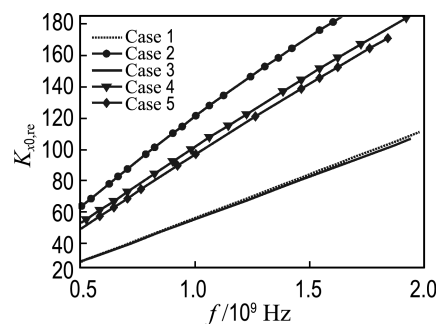
where L_d and L_w are the integration interval of k_y used in Eq. (19) and Eq. (23) respectively. Tab. 1 shows the speedup behaviors when " w " is used to accelerate the integrations. From Tab. 1 and other experiments, it is found that 10-100 times of speedup ratio can be achieved by using this window function of " w " with accuracy loss within 1%.

Tab. 1 Speedup comparison (Speedup Z_{xx}^j : Case 2 in Fig. 3 is used here with $f = 1$ GHz, $K_{x0} = 107.6 - j28.8$, $N = 4$, $M = 5$, $b = 2.0$ in Eq. (8). Widows' order $m = 1$, for window w_1 , $a = 0.3d_y$; for w_2 , $a = 0.15d_y$, d_y is defined in Eq. (8))

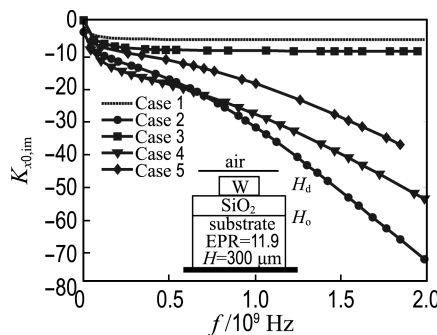
Eq. (19)	$k_y/10^6$		Speedup ratio ($\Delta Z_{xx}^j/Z_{xx}^j$)/%					
	Eq. (23)		w_1	w_2	w_1	w_2	w_1	w_2
	w_1	w_2						
Z_{xx}^0	2.117×10^2	9.6	11.0	23	20	0.080	0.083	
Z_{xx}^1	2.088×10^2	7.7	8.7	27	24	-0.070	-0.014	
Z_{xx}^2	9.763×10^1	4.8	5.3	20	19	-0.030	0.032	
Z_{xx}^3	6.960×10^1	8.7	7.7	8	9	0.001	0.057	
Z_{xx}^{11}	2.011×10^2	5.8	8.7	34	23	0.770	0.640	
Z_{xx}^{12}	1.933×10^2	4.8	11.0	40	18	-0.330	-0.280	
Z_{xx}^{13}	1.257×10^2	3.8	6.7	33	19	0.190	-0.071	
Z_{xx}^{22}	2.059×10^2	4.8	8.7	43	24	0.860	0.740	
Z_{xx}^{23}	1.943×10^2	9.6	11.0	20	18	-0.960	-0.940	

The study of complex propagation constant K_{x0} is also shown here after the new fast SDA algorithm is developed. For K_{x0} is the most important parameter of a transmission line or an on-chip interconnect. The fast algorithm is first validated by comparing it to the closed-formulas of microstrip special case. Then, for the multilayer cases, the new fast SDA algorithm results are compared to the results obtained by IE3D^[6], also compared to the measurement results^[7]. All the comparison shows the new fast algorithm works very well. After

validation, the on-chip interconnect studying with the new fast SDA algorithm focuses on CMOS interconnect lines. Fig. 3 shows 5 different cases' K_{x0} studying. Case 1 has no substrate loss, dielectric and oxide layer thicknesses are $H_d = 47 \mu\text{m}$, $H_o = 1.5 \mu\text{m}$ respectively. Interconnect is made of aluminum with cross section as $13 \mu\text{m} \times 2 \mu\text{m}$; Compared to Case 1, the only change in Case 2 is that it has substrate loss, substrate conductivity $\sigma = 10$ S/m; Case 3 is the same as Case 1, but the interconnect width W is cut by half in which $W = 6.5 \mu\text{m}$; Case 4 is the same as Case 3 but with substrate loss; case 5 is the same as Case 4, but the oxide layer thickness is doubled as $H_o = 3 \mu\text{m}$. Fig. 3 sheds very interesting lights on the loss substrate's impacting on the signal propagation: Substrate loss is much bigger than the metal loss itself in this case, but if the interconnect is far away from substrate, the substrate loss will be reduced dramatically. On the other hand, substrate loss also has impact on



(a) real part



(b) image part

Fig. 3 Propagation constant K_{x0} comparison of CMOS on-chip interconnect

the signal phase velocity, heavier substrate loss forms slower wave propagation on interconnect confirms the expectations.

4 Conclusion

A novel low-pass-filter window function (LPFW) is constructed to shorten the infinity integral interval in the traditional SDA calculation of on-chip interconnect or MMIC transmission line. Without sacrificing the accuracy, the speedup ratio can be up to 100 times in most numerical experiment cases. The proposed window-based acceleration method in the integration can be widely used due to its general outline in principle. Finally, from the engineering point of view, as $\tilde{w}(k_y)$ closed-formulation is explicitly known, so when applying Eq. (23) to the numerical integration, user can control the integration accuracy by adjusting the window's compact support easily and therefore it is good for robust coding development.

References:

[1] LEE H Y, ITOH T. Phenomenological loss equivalent method for planar quasi-TEM transmission

lines with a thin normal conductor or superconductor [J]. **IEEE Transactions on Microwave Theory and Techniques**, 1989, **37**(12):1904-1909

- [2] YU T, CAI W. High-order window functions and fast algorithms for calculating Dyadic Green's function functions in the multilayered media [J]. **Radio Science**, 2001, **36**(4):559-569
- [3] YU T, CAI W. FIFA-fast interpolation and filtering algorithm for calculating Dyadic Green's function in the EM scattering of multi-layered structures [J]. **Communication in Computational Physics**, 2006, **1**(2):229-260
- [4] MICHALSKI K, ZHENG D. Electromagnetic scattering and radiation by surfaces of arbitrary shape in layered media. I. Theory [J]. **IEEE Transactions on Antennas and Propagation**, 1990, **38**(3):335-344
- [5] YU Tie-jun, ZHANG Xue-xia, GUO Bao-xin, *et al.* The current distribution of high-Tc superconducting microstrip lines [J]. **IEEE MTT-S International Microwave Symposium Digest**, 1996, **3**:1667-1670
- [6] Vikingboy. Zeland IE3D: MoM-Based EM Simulator 14.1 [S/OL]. [2008-10-21] <http://www.mentor.com/electromagnetic-simulation>
- [7] TIEMEIJER L F, PIJPER R. On the accuracy of the parameters extracted from parameter measurements taken on differential IC transmission line [J]. **IEEE Transactions on Microwave Theory and Techniques**, 2009, **57**(6):1581-1588

基于窗口的 SDA 积分加速算法

余报楚^{*1,2}, 余庆军³, 余铁军³, 唐祯安³

- (1. 大连理工大学 工业装备结构分析国家重点实验室, 辽宁 大连 116024;
2. 大连海洋大学 土木工程学院, 辽宁 大连 116023;
3. 大连理工大学 电子科学与技术学院, 辽宁 大连 116024)

摘要: 给出了一个求解片上多层互连线的复数传播常数的谱域分析法(SDA). 由于 SDA 是一种全波分析法, 其计算量通常很大, 为了提高积分方程的求解速度, 引入了一个新颖的钟形窗口函数. 该函数在谱域内具有低通滤波特性, 并且拥有简单闭合的计算公式, 能够有效地降低计算复杂度. 基于该窗口函数的特性研究, 推导出了一个新的用于提高 SDA 积分求解速度的加速算法. 实验证明, 该算法具有较高的精度和速度.

关键词: 谱域分析法; 传输线; 介质损耗; 窗口函数; 低通滤波窗口

中图分类号: TN401 **文献标志码:** A

收稿日期: 2010-01-10; 修回日期: 2011-12-05.

基金项目: 辽宁省科学技术计划资助项目(2008217004); 中国博士后科学基金资助项目(200704111071).

作者简介: 余报楚^{*}(1974-), 男, 博士, 副教授, E-mail: baochuyu@student.dlut.edu.cn.